Time-Dependent Shear Motion in a Strongly Coupled Dusty Plasma in PK-4 on the International Space Station (ISS)

Bin Liu, John Goree, *Member, IEEE*, M. Y. Pustylnik, H. M. Thomas, V. E. Fortov, A. M. Lipaev, A. D. Usachev, O. F. Petrov, A. V. Zobnin, and M. H. Thoma

***Abstract*— Time-dependent shear motion of dust particles in a three-dimensional (3-D) strongly coupled dusty plasma under microgravity conditions was investigated using the European Space Agency–Roscosmos facility Plasma-Kristall 4 (PK-4) on the International Space Station (ISS). The dust particles, which were negatively charged, were trapped in a glow discharge plasma powered by a dc voltage that switched its polarity periodically. They self-organized themselves into a structure resembling a cold liquid. A manipulation laser beam of a circular cross section pushed a stream of particles, moving them through the surrounding sample region; its power was modulated using a rectangular pulse, causing an impulsive unsteady flow. At the onset of the impulsive motion, the flow was observed as it grew in space and time. Later, during the steady manipulation, we find the thickness of the flow region fluctuated significantly over time.**

***Index Terms*— Dusty plasma, microgravity, Plasma-Kristall 4 (PK-4), shear flows.**

I. Introduction

PLASMAS can behave like liquids or solids when they are strongly coupled [1]. A plasma is said to be strongly coupled when the interparticle potential energy greatly exceeds the kinetic energy of the constituent charged particles. In response to shear stresses, a flow pattern called shear flow can develop in a plasma in liquid state [2]–[7]. Here, we investigate shear flows that are unsteady, driven by an external force suddenly applied to a strongly coupled plasma, which in this study is a dusty plasma.

Micrometer-size dust particles in an ionized gas can make a dusty plasma that is strongly coupled [8]–[14]. When they are immersed in a typical glow discharge plasma, the dust particles can obtain a large negative charge by absorbing electrons and ions in the plasma. As in the experiment we report, the dust is charged negatively due to the greater velocity of electrons as compared to ions. Positive charges can occur in space plasmas, due to photoemission [15] or in afterglow plasmas [16], where there can be an excess of positive ions.

A collection of dust particles can be electrically confined into a three-dimensional (3-D) cloud; they can self-organize into a structural arrangement, such as liquids or solids. The particles also interact with each other through Coulomb collisions, which can cause momentum to diffuse in a velocity gradient. Shear flows of dust particles can be formed when a velocity gradient can be established across the flow direction, for example, by applying a shearing force. Here, we investigate shear flows in 3-D dusty plasmas by using a shearing force due to a manipulation laser. This dusty plasma allows video tracking of individual constituent particles, enabling a fundamental physics study at an atomic-like scale.

Dust particles can be made to flow by externally applying a small force. This is because a dusty plasma is extremely soft, with a shear modulus that is about 10^{19} times smaller than that for metals [17]–[19]. A force as small as 10^{-14} N, which can be achieved by the radiation pressure of laser light, can push particles and set them into motion. This type of particle manipulation using lasers has been applied in several dusty plasma experiments, including those under microgravity conditions [20] and those in ground-based laboratories [21], [22].

This article reports a microgravity experiment on the International Space Station (ISS). Under microgravity conditions, we observed a large dust cloud that is suitable for studying flows in 3-D. This is unlike most experiments performed on ground, where gravity causes dust to sediment in a plasma sheath. Microgravity experiments have been reported previously, including those using the international plasma microgravity facility (IMPF) chamber [23] for parabolic flight experiments, and the PKE-Nefedov [24], PK-3 Plus [25], and Plasma-Kristall 4 (PK-4) chambers [20], [26] onboard the ISS.

Manuscript received April 30, 2021; revised June 30, 2021; accepted July 19, 2021. This work was supported in part by the Deutsches Zentrum für Luft- und Raumfahrt (DLR) under Grant 50WM1441 and Grant 50WM1742; in part by the Joint Institute for High Temperatures of the Russian Academy of Sciences (JIHT RAS) funded by the Ministry of Science and Higher Education of the Russian Federation under Grant 075-00892-20-01; and in part by Iowa funded by National Aeronautics and Space Administration-Jet Propulsion Laboratory (NASA-JPL) under Contract 1579454, Contract 1573629, and Contract 1661767. The review of this article was arranged by Senior Editor T. Hyde. *(Corresponding author: Bin Liu.)*

Bin Liu and John Goree are with the Department of Physics and Astronomy, The University of Iowa, Iowa, IA 52242 USA (e-mail: bin-liu@uiowa.edu).

M. Y. Pustylnik and H. M. Thomas are with the Forschungsgruppe Komplexe Plasmen, Institut für Materialphysik im Weltraum, Deutsches Zentrum für Luft- und Raumfahrt, 82234 Weßling, Germany.

V. E. Fortov, deceased, was with the Joint Institute for High Temperatures of the Russian Academy of Sciences (JIHT RAS), 125412 Moscow, Russia.

A. M. Lipaev, A. D. Usachev, O. F. Petrov, and A. V. Zobnin are with the Joint Institute for High Temperatures of the Russian Academy of Sciences (JIHT RAS), 125412 Moscow, Russia.

M. H. Thoma is with the I. Physikalisches Institut, Justus-Liebig-Universität Gießen, 35392 Gießen, Germany.

Color versions of one or more figures in this article are available at https://doi.org/10.1109/TPS.2021.3100300.

Digital Object Identifier 10.1109/TPS.2021.3100300

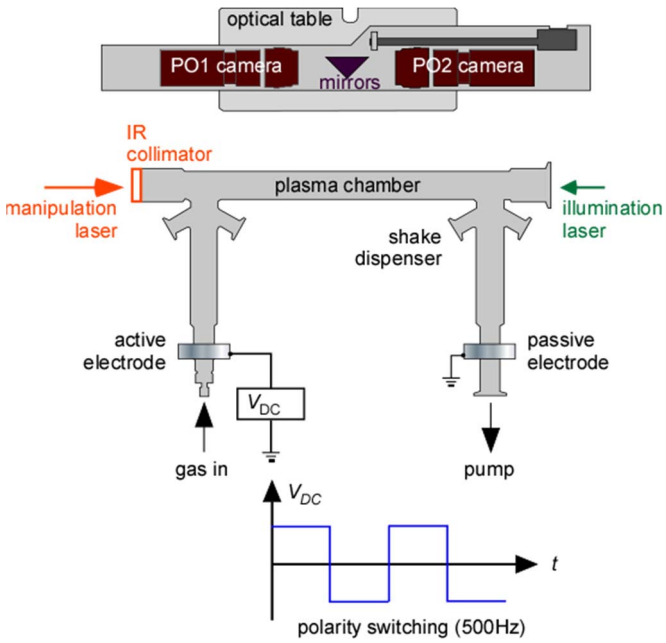

Fig. 1. PK-4 instrument. A glow discharge plasma is established in a U-shaped plasma chamber by applying dc voltages across the active and passive electrodes. To trap dust particles, which are injected into the chamber by a shaker dispenser, the polarity of the voltages was switched periodically at 50% duty cycle. A pair of particle observation (PO) cameras view a thin slab of the particles illuminated by a laser sheet. A manipulation laser beam propagates along the axis of the plasma chamber, creating a particle flow.

We investigate shear flows in a 3-D dusty plasma using PK-4 on the ISS. The PK-4 instrument has been previously used to study topics, such as velocity distribution [27], particle diffusion [28], waves [29]–[31], structures [32], and shear flows [33]. A previous experiment studying shear flows [33] yielded an estimate of viscosity, in a flow of dust particles that was steady. Here, we mainly focus on an unsteady flow, produced by a sudden application of a manipulation laser to a dust cloud. In particular, we study the spatial and temporal evolution of a transition shear layer created in the vicinity of flowing particles. We note that unsteady flows and boundary layers are of fundamental interest in fluid dynamics. Our experiment can explore these topics at a particle level, using video imaging of individual particles.

II. Experiment

Our microgravity experiment was performed using the Joint ESA-Roscosmos "Experiment Plasma Kristall-4" (PK-4) facility [20], [26], onboard the ISS. The main scientific features of the PK-4 instrument are sketched in Fig. 1. The instrument centers on a U-shaped glass plasma chamber, powered using a dc voltage applied across two electrodes, which are termed active and passive electrodes. In this experiment, a glow discharge was established in 40-Pa neon gas, with a discharge current of 0.5 mA. Using a shaker dispenser, dust particles of radius 3.43 μm were momentarily injected into the chamber. The dust particles experienced gas friction, with an Epstein damping rate of $\nu_E = 44\ \mathrm{s}^{-1}$ [13], [34].

Once entering the plasma, the dust particles became negatively charged; they drifted toward the center of the chamber, due to the dc electric field. Once they approached the center of the chamber, the polarity of the dc voltage was then periodically switched, at a frequency of 500 Hz and a duty cycle of 50%. This polarity switching trapped the particles, maintaining a steady dust cloud. The conditions of this experiment avoided self-excited waves such as dust acoustic waves [31].

To create a shear flow in the dust cloud, we used a manipulation laser to push a stream of dust particles to move through the cloud. The manipulation laser applied a radiation pressure force that was localized near a central axis of the dust. The resulting stream of moving particles served as a moving boundary and created a velocity shear among the dust particles in the region next to the laser beam. The advantage of this optical manipulation is that the radiation pressure due to the laser only pushes the dust particles but without affecting surrounding plasma conditions. A fiber-coupled diode laser (Jenoptik JOLD-30-FCM-12) [20] generated a powerful laser beam, which had a $1/e^2$ width of 1.5 mm. To excite a pulsed motion in the particle cloud, the current of the laser diode was modulated with a rectangular waveform, with a pulse duration of 11 s.

We tracked dust motion using video cameras. Two particle observation (PO) cameras were used, along with an illumination laser sheet. These cameras were aligned along the axis of the plasma chamber, with a slight overlap of their fields of view. The PO cameras viewed at 90° to the sheet-like beam from the illumination laser so that the images obtained are essentially cross-sectional images. The cameras were operated at 70 frames/s. The images recorded by the cameras are our primary experimental data; they have the dimensions 1600 × 480 pixels with 0.0142-mm/pixel resolution. Fig. 2(a) shows a cropped view of a single frame, i.e., a snapshot image of dust particles.

III. Data Analysis

A. Structure Characterization

We characterize the structure of our 3-D dust cloud using a pair correlation function $g(r)$ (see Fig. 3). This function is calculated using the method in [35] with an input of the positions of individual particles. The particle position is determined using an optimized moment method [36] with our 2-D image data, under conditions without laser manipulation.

This pair correlation function is useful for two purposes. First, it allowed us to obtain the particle spacing, 0.35 mm, and the number density of our 3-D dust cloud, $3.3 \times 10^{10}\ \mathrm{m}^{-3}$, using the method in [35]. Second, its shape allows us to confirm the strongly coupled character of our dust cloud. The height of the first peak of $g(r)$ in Fig. 3 is descriptive of the structure of a cold liquid or possibly a disordered solid.

It is significant that the dust cloud was not crystalline because this means that it was not necessary for the manipulation laser to melt a crystal, as in some ground-based experiments. The particle cloud was already in a disordered state, suitable for driving a flow that could start without a delay due to melting.

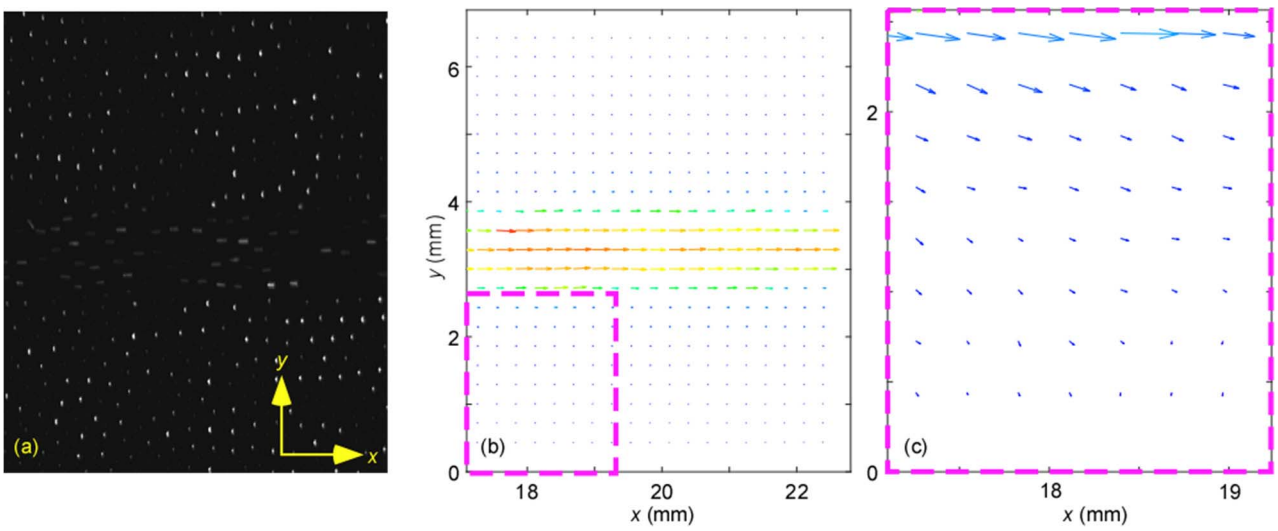

Fig. 2. (a) Snapshot image of dust particles, viewed from a PO camera. The image shown is a cropped view of a raw image, which has a field of view of 22.7 mm × 6.8 mm. The stripe-like feature near the middle of the image is due to particles that are flowing, driven by a manipulation laser propagating through the dust cloud. (b) Example velocity vector field, as calculated using PIV with image data. (c) Magnified view of a portion of (b), revealing a prevailing flow motion in the x-direction as well as a slight drift in the transverse y-directions.

B. Flow Characterization

To characterize flows in the cloud, we calculated the velocity vector field (u_x, u_y) using particle image velocimetry (PIV) [31], [37]–[39]. We first preprocessed our recorded images by subtracting a background image and enhancing the contrast of the images using histogram equalization. We then divided each preprocessed image into an array of interrogation areas of dimension 0.625 mm × 0.625 mm. The displacement in each interrogation area centered at (x, y) was evaluated using the direct cross correlation method [31], [37], [38]. This resulted in instantaneous velocity vectors (u_x, u_y) at (x, y), for the time t at the midpoint between two consecutive frames. An example of the resulting velocity vector field is shown in Fig. 2(b) and (c).

Using the resulting velocity field, we obtained the spatial profiles of the dust-fluid velocities, for both the x- and y-directions, where the flow was driven in the x-direction. The fluid velocity in the x-direction, $V_x(y, t)$, was obtained by averaging the instantaneous fluid velocity u_x over the position x. Fig. 4(a) shows the examples of $V_x(y, t)$ for different times. Similarly, we also obtained the fluid velocity $V_y(y, t)$ for transverse dust motion in the y-direction, which is perpendicular to the flow direction.

IV. Results

In this section, we report the results for our experimental observations of dust motion in response to an impulsive external force applied by the manipulation laser. In general, the laser radiation pressure force caused dust motion mainly in the x-direction and to a much less degree in the y-direction. The instantaneous velocity vector field is shown in Fig. 2(b) and (c).

Since the force applied by laser light was a pulse of long duration, we observed unsteady shear motion especially in the rising edge of the pulse, along with more steady flows during the pulse. For the longitudinal motion in the x-direction, our results characterize the transient development in the rising edge, and they reveal fluctuations during what was otherwise the steady phase. For the transverse motion in the y-direction, we also present our observations.

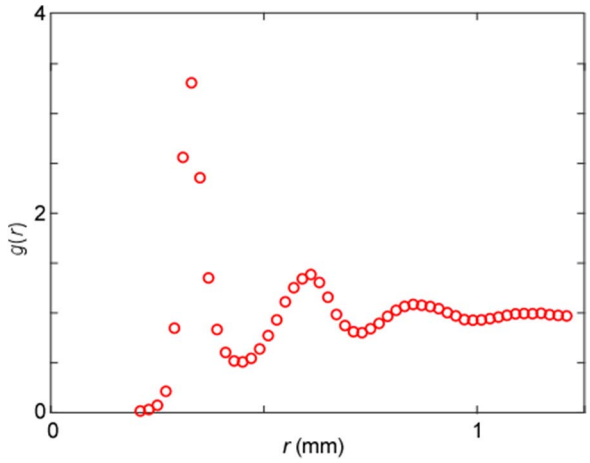

Fig. 3. 3-D pair correlation function $g(r)$, calculated using the method in [35] with individual particle position. Note that the position data are for an undisturbed dust cloud, in the absence of laser manipulation. This curve indicates that our undisturbed cloud had a liquid-like structure, with 3-D number density $n_d = 3.3 \times 10^{10}$ m^{-3}, and an interparticle distance 0.35 mm, corresponding to a Wigner–Seitz radius $(3/4\pi n_d)^{1/3} = 0.2$ mm.

A. Onset of Unsteady Shear Flows

As we turned on the manipulation laser, the impulsive dust flow initially grew rapidly and then approached a steady level. We find that this growth develops in time with an amplitude $\propto [1 - \exp(-\nu t)]$. This development of the overall flow velocity is also consistent with what would be expected for single-particle motion in the presence of a constant driving force opposed by a friction-like force with a coefficient ν.

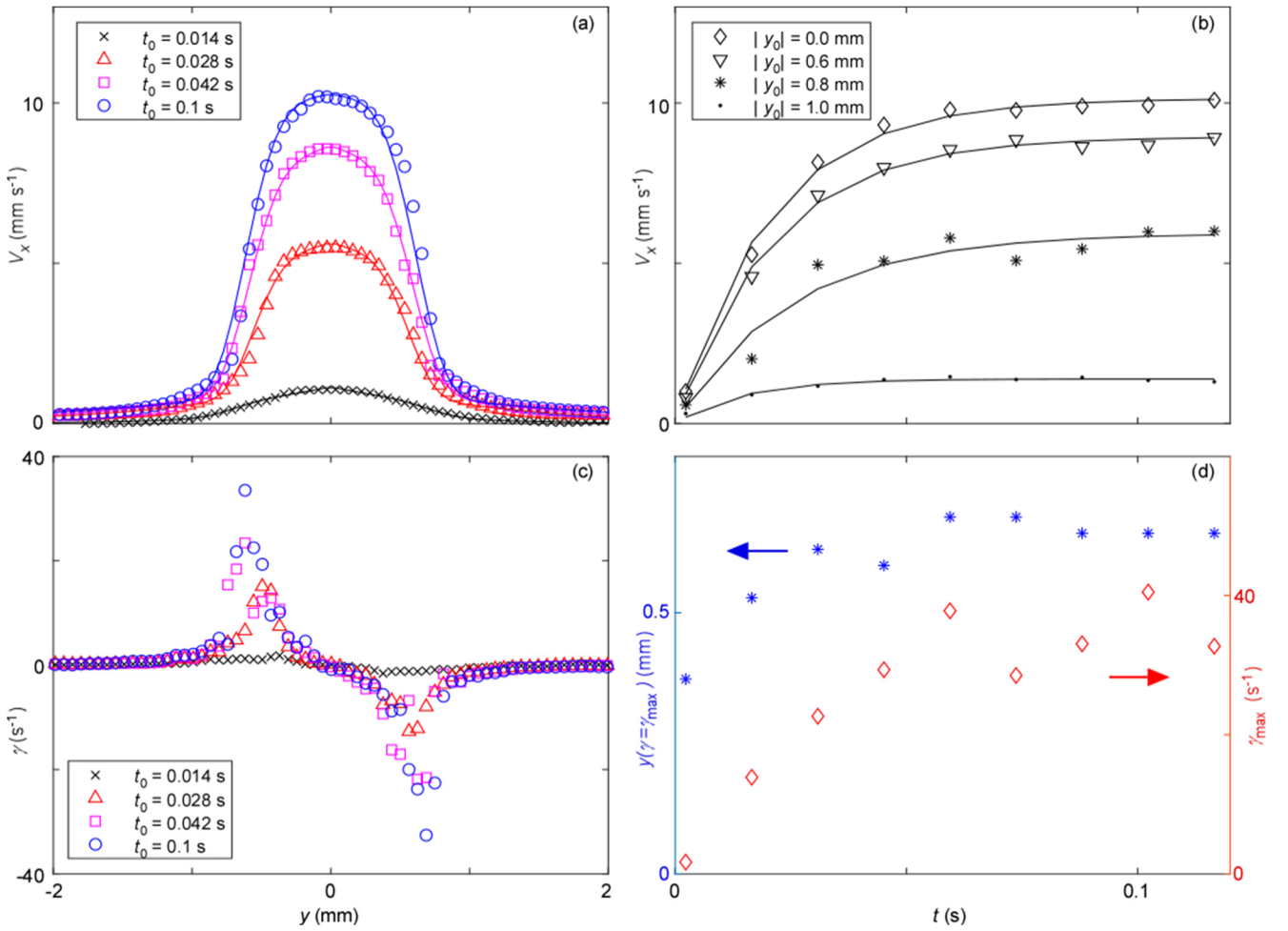

Fig. 4. Unsteady flows in dust, during an initial growth phase upon a sudden application of a manipulation laser. (a) Dust-fluid velocity V_x (y, t_0), varying with the position y across the direction of flow, at different times $t = t_0$. Data points were obtained by averaging the velocity field (u_x, u_y), such as that in Fig. 2(b), over the position x. The continuous curves in (a) fit the expression: $a\exp(-y^4/d^4)+b\exp(-y/c)$, with parameters $d = 0.67$ mm, $c = 1.09$ mm, as well as a and b which increase with time during the rising edge of the pulse. (b) Temporal growth of dust-fluid velocity, $V_x(y_0, t)$, at different locations $y = y_0$ from the central axis of the manipulation laser beam. The continuous curves in (b) fit the expression $\propto 1-\exp(-\nu t)$, with $\nu = 51$ s^{-1} as a free parameter. (c) Shear rate γ, obtained by calculating the derivative of the velocity profile in (a) with respect to y. (d) Maximum shear rate (◇) and the location where the maximum occurs (*), as obtained from (c).

To reveal the initial growth of dust flow, we present the dust-fluid velocity as a function of time in Fig. 4(b). The data shown are for four different y locations from the axis of the manipulation laser beam. All the data show a rapid growth at short time. To quantify this growth, we fit the data to the expression $\propto [1-\exp(-\nu t)]$, with ν as a free parameter. We find that the fitted coefficient has a value $\nu = 51 \pm 12$ s^{-1}; this experimental value is comparable to the theoretical frictional coefficient due to neutral gas, $\nu_E = 44$ s^{-1}.

Our result in Fig. 4(b), in which the flow velocity develops as $\propto [1-\exp(-\nu t)]$, indicates that the initial evolution is mostly determined by gas friction. This is characterized by a rate of growth ν on the gas-friction time scale. This result for the temporal development of our unsteady flow is consistent with the findings for the spatial profile of a steady flow [33], where the authors found that the shape of the steady flow profiles was mostly dominated by gas friction.

The time-dependent flow pattern is characterized in Fig. 4(a), exhibiting the spatial and temporal growth of the dust-fluid velocity immediately after the laser was turned on. Velocity profiles are presented for four times. In general, the shape of these velocity profiles in Fig. 4(a) exhibits a broad top near the axis of the laser beam, for $y \approx 0$, and along with a strong gradient in a transitional layer near the edge of the laser beam, for $|y| \approx 0.5$ mm. We find that the observed profile can be fitted to the expression: $a\exp(-y^4/d^4) + b\exp(-y/c)$, with the parameters: $d = 0.67 \pm 0.06$ mm, $c = 1.09 \pm 0.30$ mm, as well as a and b that increase with time during the rising edge of the pulse. The fitted data are shown as the continuous curves in Fig. 4(a). Our fitting here is slightly different from that in [33], but it is motivated by the previous article. The slight modification in our expression is better for fitting our data at large y.

We note that the velocity profile here is determined by a combination of two factors: the intensity profile of the manipulation laser and the viscosity of our dust cloud. In [33], an estimate for viscosity in PK-4, in the range of 0.2–6.7 mm^2/s, was obtained under steady flow conditions.

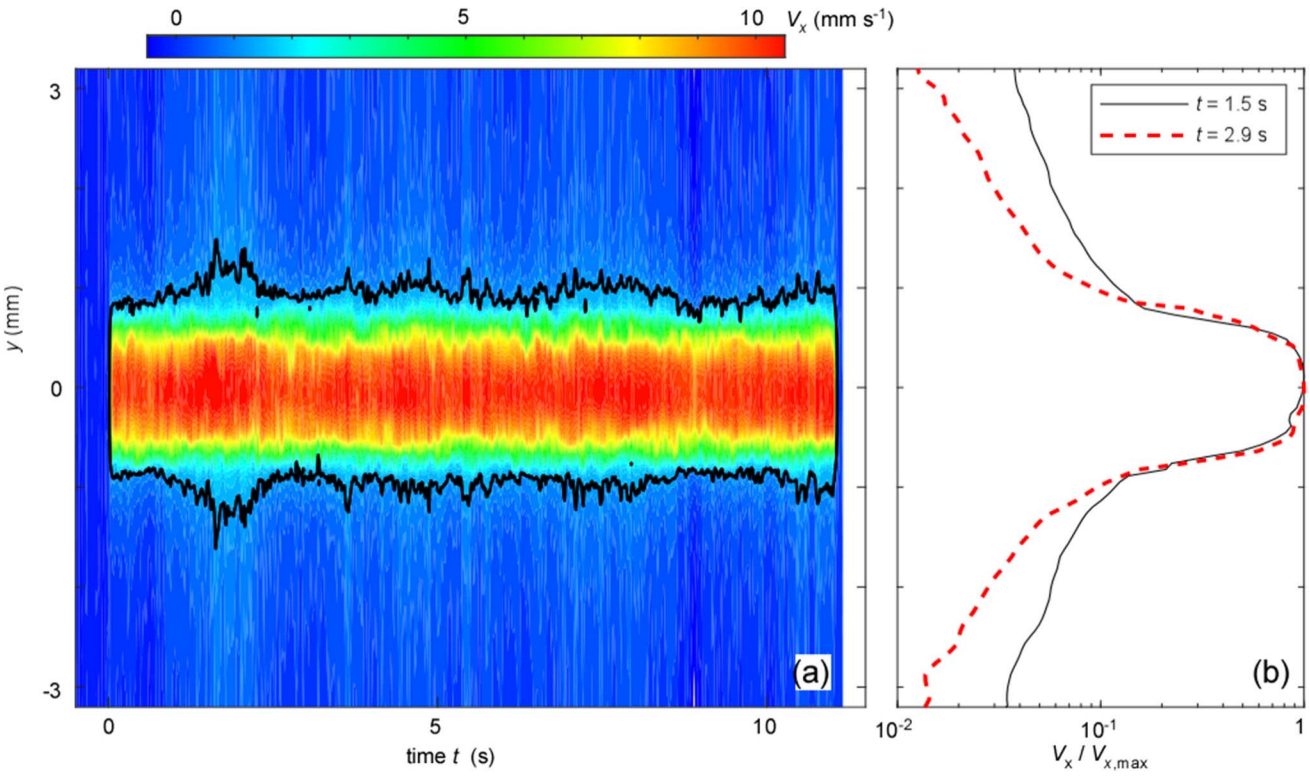

Fig. 5. (a) Space–time diagram of dust-fluid velocity $V_x(y, t)$. Color indicates the amplitude of the velocity. The solid line in (a) marks the contour level at $V_x \approx 1$ mm/s, showing fluctuations of flow pattern, which have different characters in different spatial regions. At the edges, i.e., the transitional low-gradient region, there are significant fluctuations that are largely symmetric for $+y$ versus $-y$. Nearer the center, in the high-gradient region at $|y| \approx 0.3$ mm, the fluctuations are asymmetric, suggesting different underlying mechanisms in these two regions. (b) Dust-fluid velocity profiles at two moments in time, indicating a significant change in the shape of the velocity profile, even though the experimental conditions were held steady.

To reveal shear motion, in Fig. 4(c), we present the shear rate γ variation across the flow in the y-direction. The shear rate was calculated as the derivative of the velocity profile in Fig. 4(a), with respect to y. Results in Fig. 4(c) show that the shear rate has two extreme values, near the edges of the laser beam. The maximum shear rate, along with its location, is presented in Fig. 4(d).

We find that the shear rate exhibits an initial growth with time. This is seen from the maximum shear rate as a function of time in Fig. 4(d). We also find that the shear layer expands initially, as indicated by the location for the maximum moving away from the laser beam.

B. Flow Fluctuation During Steady Manipulation

Here, we characterize flow fluctuations during the steady manipulation. We will show different characteristics of the fluctuations in different spatial domains of the manipulated dust cloud. During the steady laser manipulation, three different domains were observed in the dust cloud. A region of rapid flow was formed inside the laser beam, $|y| < 0.5$ mm, where particles exhibited fast drift, with a fluid velocity about 10 mm/s. Near the edge of the manipulation laser beam, $0.5 < |y| < 1.5$ mm, a transitional shear layer was observed, with a large gradient, i.e., shear rate. Far from the laser beam, $|y| > 1.5$ mm, there was a nearly undisturbed domain, which retained essentially the same microscopic structure, as in the absence of any manipulation, except that particles in this undisturbed domain still exhibited a small drift (<1 mm/s).

1) Fluctuations of Shear Flow Patterns: Fig. 5(a) shows a space–time diagram of dust-fluid velocity $V_x(y, t)$. This plot reveals significant fluctuations. To draw attention to fluctuations in the transition shear layer, a heavy contour line is drawn at $V_x \approx 1$ mm/s.

To further reveal this fluctuation, we also show the instantaneous velocity profiles at two moments in time, in Fig. 5(b), plotted in semilogarithmic scale. At large distances, $|y| > 1$ mm, velocity profile varies greatly with time, even though the experiment conditions were held the same.

The flow fluctuations exhibited different characteristics in different spatial domains of the dust cloud. In particular, we note a different kind of symmetry: fluctuations are symmetric about the central axis for $|y| \geq 1$ mm, but unsymmetric for the high-gradient region at $|y| \approx 0.3$ mm.

In the high-gradient region at $|y| \approx 0.3$ mm, the spatial excursion of the fluctuation is comparable to the particle spacing, which was about 0.35 mm. This size suggests that this fluctuation was local and arises from a particle–particle interaction. Presumably, particles just outside the flow region scatter from rapidly moving particles as they pass by, just within the flow.

In the low-gradient region at $|y| \geq 1$ mm, the edge of the transitional shear layer exhibited fluctuations, as highlighted by the heavy contour lines in Fig. 5(a). Two points that we note especially are: the symmetry of these contour lines and the separation of the contours which is significantly greater than the interparticle distance. Due to this great distance, the correlation

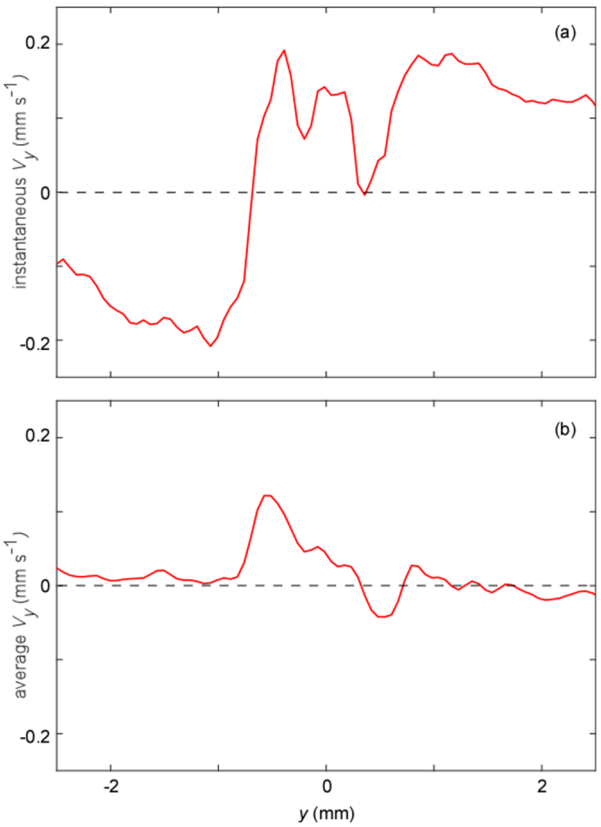

Fig. 6. Profiles of the transverse velocity, in the y-direction: (a) Instantaneous velocity $V_y(y, t)$ during the flow's onset at $t = 0.07$ s, indicating an outward particle flow away from the central beam during the onset of the shear flows. (b) Time-averaged velocity, during steady manipulation, exhibiting a transverse flow localized mainly inside the laser beam. The two extrema in (b) coincide with those for the shear rate in Fig. 4(c).

in the fluctuations must not be from a local particle–particle collision but from a macroscopic or fluid effect. The laser intensity profile and gas friction were expected to be steady during the time interval of interest, yet there is nevertheless a significant fluctuation at hydrodynamic distances. We are unsure of the exact character of this hydrodynamic fluctuation.

2) Transverse Motion: Here, we comment upon our observations of the transverse motion. In addition to a prevailing flow in the x-direction, a transverse motion in the y-direction was also observed.

During the onset of flow, when the laser is turned on, Fig. 6(a) shows the transverse velocity profile. This graph indicates an outward flow of particles, away from the central axis of the laser beam. We find that this transverse flow was transient. It only occurred during the onset of the shear flow, and it reached its maximum at $t \approx 0.07$ s.

During the steady laser manipulation, we find that the transverse motion was mostly localized inside the laser beam. This is seen from the transverse velocity profile in Fig. 6(b), which was obtained by averaging the instantaneous velocity profile $V_y(y, t)$ over the time interval $1 \leq t \leq 10$ s. From Fig. 6(b), the transverse motion was directed toward the central axis; it was mostly significant near the locations where the shear rate had its extreme values. This coincidence might suggest a role for viscous heating, which can scatter flow energy in the x-direction to the transverse y-direction.

V. Summary

We presented a microgravity experiment using the ESA-Roscosmos facility PK-4 on the ISS, investigating time-dependent shear motion in 3-D dusty plasmas. In particular, we characterized the onset of unsteady shear flows when we turned on a manipulation laser and the fluctuations in flow patterns during the steady laser manipulation.

A strongly coupled dusty plasma was trapped in a glow discharge plasma. Using dc voltage with polarity switching, we produced a plasma in low-pressure neon. Dust particles were confined into a large-volume 3-D cloud, exhibiting a structural arrangement like a cold liquid.

A manipulation laser, which was modulated by a rectangular waveform, drove an impulsive unsteady particle flow near the center of the cloud. At the onset of the impulsive motion, the fluid velocity was observed to grow in space and time. During the steady laser manipulation, we find that the flow fluctuated significantly over time, with a different character for the fluctuations in the high-gradient region compared to outlying regions. In the direction transverse to the prevailing flow direction, the laser manipulation also caused a detectable transverse motion.

Future work that could be performed using experiments like ours includes the study of fundamental physics problems such as momentum transport and viscous heating in a 3-D dusty plasma. These phenomena have been observed previously in a 2-D dusty plasma [18]. Another possible topic for future work is the excitation of acoustic waves by an impulsive shear flow, as has been predicted by simulation for 3-D dusty plasmas [41].

Acknowledgment

The authors recall Vladimir Ivanovich Molotkov, who passed away on July 11, 2019, and did so much for the International Space Station (ISS) complex plasma program. They would like to thank the joint ESA/Roscosmos "Experiment Plasmakristall-4" onboard the ISS.

References

[1] G. J. Kalman, K. B. Blagoev, and M. Rommel, *Strongly Coupled Coulomb Systems*. New York, NY, USA: Plenum Press, 1998.
[2] V. Nosenko and J. Goree, "Shear flows and shear viscosity in a two-dimensional Yukawa system (dusty plasma)," *Phys. Rev. Lett.*, vol. 93, no. 15, Oct. 2004, Art. no. 155004.
[3] A. Gavrikov, I. Shakhova, A. Ivanov, O. Petrov, N. Vorona, and V. Fortov, "Experimental study of laminar flow in dusty plasma liquid," *Phys. Lett. A*, vol. 336, nos. 4–5, pp. 378–383, Mar. 2005.
[4] A. V. Gavrikov *et al.*, "Investigation of non-newtonian behavior of dusty plasma liquid," *J. Plasma Phys.*, vol. 76, nos. 3–4, pp. 579–592, Aug. 2010.
[5] C.-L. Chan, C.-W. Io, and L. I, "Dynamical heterogeneities in 2D dusty plasma liquids at the discrete level," *Contrib. Plasma Phys.*, vol. 49, nos. 4–5, pp. 215–234, Jun. 2009.
[6] W.-Y. Woon and I. Lin, "Defect turbulence in quasi-2D creeping dusty-plasma liquids," *Phys. Rev. Lett.*, vol. 92, no. 6, Feb. 2004, Art. no. 065003.
[7] Y. Feng, J. Goree, and B. Liu, "Evolution of shear-induced melting in a dusty plasma," *Phys. Rev. Lett.*, vol. 104, no. 16, Apr. 2010, Art. no. 155003.

[8] H. Thomas, G. E. Morfill, V. Demmel, J. Goree, B. Feuerbacher, and D. Möhlmann, "Plasma crystal: Coulomb crystallization in a dusty plasma," *Phys. Rev. Lett.*, vol. 73, no. 5, pp. 652–655, Aug. 1994.

[9] J. H. Chu and I. Lin, "Direct observation of Coulomb crystals and liquids in strongly coupled RF dusty plasmas," *Phys. Rev. Lett.*, vol. 72, no. 25, pp. 4009–4012, Jun. 1994.

[10] A. Melzer, A. Homann, and A. Piel, "Experimental investigation of the melting transition of the plasma crystal," *Phys. Rev. E, Stat. Phys. Plasmas Fluids Relat. Interdiscip. Top.*, vol. 53, no. 3, pp. 2757–2766, Mar. 1996.

[11] W.-T. Juan and I. Lin, "Anomalous diffusion in strongly coupled quasi-2D dusty plasmas," *Phys. Rev. Lett.*, vol. 80, no. 14, pp. 3073–3076, Apr. 1998.

[12] K. Qiao and T. W. Hyde, "Structural phase transitions and out-of-plane dust lattice instabilities in vertically confined plasma crystals," *Phys. Rev. E, Stat. Phys. Plasmas Fluids Relat. Interdiscip. Top.*, vol. 71, no. 2, Feb. 2005, Art. no. 026406.

[13] A. Kananovich and J. Goree, "Shocks propagate in a 2D dusty plasma with less attenuation than due to gas friction alone," *Phys. Plasmas*, vol. 27, no. 11, Nov. 2020, Art. no. 113704.

[14] M. Bonitz, C. Henning, and D. Block, "Complex plasmas: A laboratory for strong correlations," *Rep. Prog. Phys.*, vol. 73, no. 6, May 2010, Art. no. 066501.

[15] C. K. Goertz, "Dusty plasmas in the solar system," *Rev. Geophys.*, vol. 27, no. 2, pp. 271–292, May 1989.

[16] L. Couëdel, A. A. Samarian, M. Mikikian, and L. Boufendi, "Dust charge distribution in complex plasma afterglow," *EPL Europhysics Lett.*, vol. 84, no. 3, p. 35002, Nov. 2008.

[17] A. Melzer and J. Goree, *Low Temperature Plasmas: Fundamentals, Technologies and Techniques*, 2nd ed., R. Hippler, H. Kersten, M. Schmidt, and K. H. Schoenbach, Eds. Weinheim, Germany: Wiley-VCH, 2008, p. 129.

[18] Y. Feng, J. Goree, and B. Liu, "Observation of temperature peaks due to strong viscous heating in a dusty plasma flow," *Phys. Rev. Lett.*, vol. 109, no. 18, Oct. 2012, Art. no. 185002.

[19] B. Liu and J. Goree, "Determination of yield stress of 2D (Yukawa) dusty plasma," *Phys. Plasmas*, vol. 24, no. 10, Oct. 2017, Art. no. 103702.

[20] M. Y. Pustylnik *et al.*, "Plasmakristall-4: New complex (dusty) plasma laboratory on board the international space station," *Rev. Scientific Instrum.*, vol. 87, no. 9, Sep. 2016, Art. no. 093505.

[21] V. Nosenko, J. Goree, and A. Piel, "Laser method of heating monolayer dusty plasmas," *Phys. Plasmas*, vol. 13, no. 3, Mar. 2006, Art. no. 032106.

[22] Z. Haralson and J. Goree, "Temperature dependence of viscosity in a two-dimensional dusty plasma without the effects of shear thinning," *Phys. Plasmas*, vol. 23, no. 9, Sep. 2016, Art. no. 093703.

[23] A. Piel, M. Klindworth, O. Arp, A. Melzer, and M. Wolter, "Obliquely propagating dust-density plasma waves in the presence of an ion beam," *Phys. Rev. Lett.*, vol. 97, no. 20, Nov. 2006, Art. no. 205009.

[24] A. P. Nefedov *et al.*, "PKE-Nefedov*: Plasma crystal experiments on the international space station," *New J. Phys.*, vol. 5, p. 33, Apr. 2003.

[25] H. M. Thomas *et al.*, "Complex plasma laboratory PK-3 plus on the international space station," *New J. Phys.*, vol. 10, no. 3, Mar. 2008, Art. no. 033036.

[26] A. D. Usachev *et al.*, "Influence of dust particles on the neon spectral line intensities at the uniform positive column of dc discharge at the space apparatus 'plasma Kristall-4,"' *J. Phys., Conf. Ser.*, vol. 946, Feb. 2018, Art. no. 012143.

[27] B. Liu *et al.*, "Particle velocity distribution in a three-dimensional dusty plasma under microgravity conditions," in *Proc. AIP Conf.*, vol. 1925, Jan. 2018, Art. no. 020005.

[28] Z. Wei *et al.*, "Diffusive motion in a 3-D cluster in PK-4," *IEEE Trans. Plasma Sci.*, vol. 47, no. 7, pp. 3100–3106, Jul. 2019.

[29] S. Jaiswal *et al.*, "Dust density waves in a DC flowing complex plasma with discharge polarity reversal," *Phys. Plasmas*, vol. 25, no. 8, Aug. 2018, Art. no. 083705.

[30] V. V. Yaroshenko *et al.*, "Excitation of low-frequency dust density waves in flowing complex plasmas," *Phys. Plasmas*, vol. 26, no. 5, May 2019, Art. no. 053702.

[31] J. Goree *et al.*, "Correlation and spectrum of dust acoustic waves in a radio-frequency plasma using PK-4 on the international space station," *Phys. Plasmas*, vol. 27, no. 12, Dec. 2020, Art. no. 123701.

[32] M. Y. Pustylnik *et al.*, "Three-dimensional structure of a string-fluid complex plasma," *Phys. Rev. Res.*, vol. 2, no. 3, Aug. 2020, Art. no. 033314.

[33] V. Nosenko *et al.*, "Shear flow in a three-dimensional complex plasma in microgravity conditions," *Phys. Rev. Res.*, vol. 2, no. 3, Sep. 2020, Art. no. 033404.

[34] B. Liu, J. Goree, V. Nosenko, and L. Boufendi, "Radiation pressure and gas drag forces on a melamine-formaldehyde microsphere in a dusty plasma," *Phys. Plasmas*, vol. 10, no. 1, pp. 9–20, Jan. 2003.

[35] B. Liu, J. Goree, and W. D. S. Ruhunusiri, "Characterization of three-dimensional structure using images," *Rev. Sci. Instrum.*, vol. 86, no. 3, Mar. 2015, Art. no. 033703.

[36] Y. Feng, J. Goree, and B. Liu, "Accurate particle position measurement from images," *Rev. Scientific Instrum.*, vol. 78, no. 5, May 2007, Art. no. 053704.

[37] M. Raffel, C. E. Willert, F. Scarano, C. J. Kähler, S. T. Wereley, and J. Kompenhans, *Particle Image Velocimetry: A Practical Guide*, 3rd ed. Cham, Switzerland: Springer, 2018.

[38] W. Thielicke and E. J. Stamhuis, "PIVlab—Towards user-friendly, affordable and accurate digital particle image velocimetry in MATLAB," *J. Open Res. Softw.*, vol. 2, no. 1, p. e30, Oct. 2014.

[39] J. D. Williams, "Application of particle image velocimetry to dusty plasma systems," *J. Plasma Phys.*, vol. 82, no. 3, Jun. 2016, Art. no. 615820302.

[40] J.-P. Hansen and I. R. McDonald, *Theory of Simple Liquids*. 4th ed., Oxford, U.K.: Elsevier, 2013.

[41] B. Liu and J. Goree, "Coupling of an acoustic wave to shear motion due to viscous heating," *Phys. Plasmas*, vol. 23, no. 7, Jul. 2016, Art. no. 073707.